Performance Analysis of a Two–Stage Spectrum Sensing Scheme for Dynamic Spectrum Access in TV Bands

Domenico Capriglione, Gianni Cerro, Luigi Ferrigno, Gianfranco Miele

PII: S0263-2241(18)31165-5
DOI: https://doi.org/10.1016/j.measurement.2018.12.020
Reference: MEASUR 6154

To appear in: *Measurement*

Please cite this article as: D. Capriglione, G. Cerro, L. Ferrigno, G. Miele, Performance Analysis of a Two–Stage Spectrum Sensing Scheme for Dynamic Spectrum Access in TV Bands, *Measurement* (2018), doi: https://doi.org/10.1016/j.measurement.2018.12.020

Performance Analysis of a Two–Stage Spectrum Sensing Scheme for Dynamic Spectrum Access in TV Bands

Domenico Capriglione[a], Gianni Cerro[b], Luigi Ferrigno[b], Gianfranco Miele[b,1]

[a]Department of Industrial Engineering, University of Salerno, via Giovanni Paolo II, 84084 Fisciano, Italy,
[b]Department of Electrical and Information Engineering, University of Cassino and Southern Lazio, via G. Di Biasio, 43, 03043 Cassino, Italy

Abstract

Spectrum Sensing schemes in Cognitive Radio systems are fundamental elements for a complete opportunistic communication technology. They usually reveal the presence of occupied bands without performing a measurement of the spectrum portion actually occupied. Considering that the final aim of Cognitive Radios is the exploitation, in the most efficient way, of the spectrum holes left free by primary users, the measurement of the actual occupied spectrum becomes a fundamental task. In this framework, this paper proposes a two–stage spectrum sensing method, tailored to work in TV bands, offering a good detection of the occupied bands with selectable false alarm rates (Stage 1) and an accurate measurement of the real occupied spectrum (Stage 2). Performance results, achieved in simulation and emulation environments, prove the method's goodness and robustness to non–idealities of real acquisition systems. A comparison, with another two–stage method available in literature, has confirmed its efficacy in real contexts.

Keywords: Spectral Measurements; Cognitive Radio; Radio frequency; TV White Space (TVWS); W–RAN; Frequency–domain analysis.

1. Introduction

Every day millions of people are logged into the Internet to keep up with the news, listening web radios, watching web TVs, to manage their business or financial investments and for communication purposes. For these reasons, the diffusion of Internet access is a very important need for the common users and also for the providers of these services in order to reach even more customers. This is generally true but it is fundamental for developing and least developed countries (LDCs), because the percentage of individuals, that live in these countries, using the Internet is only 41.3% and the 17.5% [1]. A big gap respect to the developed countries in which this percentage is 81%. The reasons of this scarce diffusion of the Internet access are several, but one of the main reasons is related to the presence in these countries of wide rural areas. In these areas and in general in areas with low population density, to build telecommunication infrastructure, able to provide a broadband network coverage, has a very low economic efficiency ratio. As a consequence, taking into account the importance of a broadband Internet access as a possible developing factor for these countries, it is important to tackle this problem identifying optimal strategies and technologies that could grant a very good connectivity and, at the same time, cheap fares for the user and fast return on investment for network providers when they will be implemented. Taking into consideration the economic constraints reported in [2], wired communication technologies cannot be adopted, especially in rural areas with very low population density [3]. Regarding wireless technologies, they seem to be more suitable to this aim, but the main problem is the spectrum scarcity. In fact, radio spectrum resource is very crowded and to find free bands, to allocate for this service, is very difficult. Fortunately many studies about the spectral efficiency of the traditional frequency allocation policy in main cities of different countries, in urban and rural areas [4–10], have highlighted that some bands are heavily exploited but other bands are not in use or used for only a portion of the time. As a consequence, a possible solution could be the adoption of a Dynamic Spectrum Access (DSA) approach that allows the exploita-

*I am corresponding author

Email addresses: `dcapriglione@unisa.it` (Domenico Capriglione), `g.cerro@unicas.it` (Gianni Cerro), `ferrigno@unicas.it` (Luigi Ferrigno), `g.miele@unicas.it` (Gianfranco Miele)

tion of frequency bands, allocated for specified services, and not currently used by their licensed users (*Primary Users or PUs*). Among the several bandwidths, VHF and UHF bands, traditionally used for TV broadcasting, are the most promising thanks to their good propagation characteristics that allow to cover very large areas with a single base station (BS). Thanks to these good features many national regulators have supported the possibility to use vacant channels or frequency in these bands, called TV White Spaces (TVWSs), for unlicensed wireless network implementations. Many are the attempts to accomplish this task, one of the most promising is a standard approved by IEEE in 2011 and called IEEE 802.22 [11]. It specifies MAC and PHY layers of a Wireless Regional Area Network (W–RAN) that operates in VHF and UHF bands. It promises to reach a maximum data–rate close to 23 Mbit/s and coverage area with a radius of 30 km with a single BS. Recently, many trials have been carried out in different countries, especially in Japan [12] and India[13], demonstrating the potentiality of this standard. Furthermore, research community in measurement and communication fields is currently working on a new standard proposal, namely IEEE 802.22.3 [14], with the aim of developing the specification a Spectrum Characterization and Occupancy System as a fundamental support for the implementation of a dynamic spectrum access policy. Of course, to make possible the use of TVWSs and to really enhance the efficiency in the spectrum usage, very straightforward spectrum sensing methods have to be developed with the aim of satisfying some important and often contrasting requirements, as (i) capability of detecting the presence of PUs also with unfavorable SNR, (ii) high promptness in detecting a PU which starts to occupy the channel previously left free, (iii) capability of measuring with good accuracy and resolution the frequency range occupied by PUs. In this framework, several sensing methods have been proposed in literature taking into account different applications and hardware resources [15–20].

The authors, stemming from their past experience in the development and characterization of digital signal processing methods for spectrum sensing [21–24] and frequency agility in CR networks [25] and being an active part of the standard committee[14], propose a two–stage spectrum sensing method for dynamic spectrum access in TVWS. It has been developed in order to support every cognitive standard that is going to operate in VHF and UHF bands with particular regard to IEEE 802.22.3 system typology. The first stage offers a good detection of the occupied bands and is characterized by a low computational burden. The second stage measures the real occupied spectrum. Dependently on the accuracy requirements and the promptness degrees required by the context, the user has the possibility to select to carry out a fast analysis (rough occupied frequency band measurement) or a slow analysis (accurate occupied frequency band measurement). For example, when a DSA communication is already on, it could be useful to use a coarse sensing stage to detect primary activity restart and leave the channel in the shortest possible time. On the other way around, when a Cognitive Device wants to start an opportunistic communication (frequency agility), the fine occupied frequency band measurement could be necessary to appreciate also small frequency holes, which are undetectable by Stage 1, due to its limited frequency resolution.

The peculiarities of this method respect to other methods available in literature [26–30] are the selectable trade–off between frequency measurements accuracy and promptness, the capability to provide good results on a single and fast acquisition, the possibility to have a-priori tunable false alarm rates. In detail, the first stage of the proposed method, operates according to an energy detection scheme (that is the fastest and lightest spectrum sensing method available in literature) in a wide–band manner, by digitally filtering different channels and giving as output the occupied frequency bands without any a–priori information. Another paper in literature [31] also adopts a similar approach with respect to the presented Stage 1, but it employs sub–band widths that are equal to channel bandwidth (in DVB–T case it could be 6, 7 or 8 MHz wide) and gives binary output for each of the considered spectrum portion, thus forcing the sensing resolution to be the channel bandwidth.

On the other way around, the authors employs a uniform sub–band division, where each spectrum sub–portion is 1.45 MHz wide, in order to be able to detect both primary users, that are typically present in the VHF and UHF bands (DVB–T and Wireless microphones) and not only DVB–T users, that could be easily detected also with a 6 MHz informed channelization.

The second stage of the proposed method measures the real occupied bandwidth through a “bin by bin” analysis, instead of other methods that calculate the occupied bandwidth based on the sub-bands frequency widths.

The importance of second stage is also crucial when other secondary users must be detected in order to avoid interference to them. In this case, no *a priori* knowledge is available about channelization and carrier frequency positions and a detailed analysis (bin–based resolution) is the best to do to be accurate in detection and sensitive to low transmission powers.

Both stages proposed novelties for the proposed method respect to those presents in literature.

The adoption of wide-band energy detection in frequency domain (for the Stage 1) and the real occupied bandwidth (for the stage 2) represent the biggest novelties of the method. Looking at the realization of the measurement instrument that could implement the proposed algorithm (as sensor devices described inside the draft specifications in [14]), another key aspect is that the method allows employing a light stage in the RF acquisition section avoiding the need to have very narrow band–pass, fixed or variable, filters. In addition, the proposed method does not require any theoretical assumption on the noise variance, since it is directly measured on a surely vacant channel. Finally, as shown in the following, it requires a single shot acquisition with a limited number of samples to allow appreciable results.

The method analysis and its performance assessment have been carried out in two phase: simulation, where the algorithm has been tuned and make suitable to achieve the target performance and through an experimental measurement campaign on emulated signals, where the proposed method and its robustness to non–idealities of real hardware and generation instruments have been validated.

The paper is organized as follows: the problem statement is discussed in Section 2, while the proposed method is reported in Section 3 and the performance assessment is provided in Section 4. A comparison with another sensing method is provided in Section 5 and conclusions follow in Section 6.

2. The problem statement

In order to efficiently use the spectrum and protect licensed users from harmful interference by secondary transmitters, i.e. Cognitive Radio devices, a crucial phase of the Cognitive Cycle is represented by the Spectrum Sensing (SS) task. It can be defined as an hypothesis test problem, i.e. for a given frequency interval under analysis, the SS method has to perform a binary decision about the presence/absence of an active user in such frequency span. In other words, it has to classify the analyzed spectrum portion as occupied or free by incumbent users. This problem can be formulated according to detection theory principles.
Let $y(t)$ the received signal at time instant t. It can be described as:

$$y(t) = \begin{cases} s(t) + w(t), & \text{under } H_1 \ \ hyp. \\ w(t), & \text{under } H_0 \ \ hyp. \end{cases}, \tag{1}$$

where $s(t)$ and $w(t)$ represent the transmitted signal and the noise realization, respectively. H_0 and H_1 hypothesis describes the free and occupied channel cases, respectively.

The detection problem can be reduced to the identification of the best hypothesis according to the received signal $y(t)$.

Possible solutions are:

- Output H_0 under H_0 condition (case 1) $\Longrightarrow$ $P(H_0 \mid H_0) > P(H_1 \mid H_0)$;
- Output H_1 under H_1 condition (case 2) $\Longrightarrow$ $P(H_1 \mid H_1) > P(H_0 \mid H_1)$;
- Output H_1 under H_0 condition (case 3) $\Longrightarrow$ $P(H_1 \mid H_0) > P(H_0 \mid H_0)$;
- Output H_0 under H_1 condition (case 4) $\Longrightarrow$ $P(H_0 \mid H_1) > P(H_1 \mid H_1)$;

where $P(H_i \mid H_j)$ indicates the conditional probability for the event H_i given the H_j condition satisfaction.
In cases 1 and 2 the problem is correctly solved, while cases 3 and 4 can be defined "false alarm" and "missed detection", respectively.

Several techniques are proposed in literature to solve such problem. The main categorization is among *blind* and *informed* techniques. The former methods do not exploit any *a priori* information about the signal typology to be detected, the channelization of the frequency span to be analyzed, resulting in a wider applicability range. The latter techniques are specifically tailored on particular signal shapes and typologies, exploit *a priori* knowledge about signal features and such information allow them to be more effective in difficult operating scenarios. Sensing techniques such as energy detection, wavelet–based detection and Maximum–Minimum Eigenvalue (MME) belong to blind category, whilst matched–filter, cyclostationarity and waveform based detection are in the informed techniques subset. Further subdivisions concern the application domain of each technique (time, frequency) and the spectrum interval width under analysis (narrow–band, wide–band).
Informed techniques usually provide binary information about the presence/absence of the specific user they are developed for, while blind techniques' output needs additional information, such as user bandwidth and exact edge locations, just to cite the strictly needed pieces of data.
The main goal of this work is to present a two–stage wideband spectrum sensing technique having semi–informed features, i.e. developed for well–performing

in TVWS, but able to detect very different typologies of signals, such as DTV broadcasters and Wireless Microphones (WMs).
According to its detection capabilities, the presented sensing method can be used as support by actors involved in DSA access in TVWS, as IEEE 802.22s [11].
Furthermore, a secondary goal is to provide a tunable computational burden method, able to be run in low–cost or high performance scenarios, with variable accuracy and resolution levels.
Finally, a real–scenario test set–up is also presented, to verify the robustness of the described method to real signals, where ideal hypotheses can not always be considered as valid, due to the use of real generation and acquisition instrumentation.

3. Proposal

The proposed method is divided into two stages: the first stage consists of the implementation of an energy detection method in frequency domain, where a uniform segmentation process of the analyzed spectrum is carried out to perform sub–band accurate detection; the second stage is a refinement algorithm, taking as input the sub–bands declared as occupied by the Stage 1 and refining the output results, in order to have a bin–level resolution and exploit also within–sub–band spectrum holes. Following this approach, the method presents two different exit points: the coarse results of first Stage procedure and the fine and improved output of the overall technique. According to different needs of the target application and its computational capabilities, it is possible to extract first or second set of data.

3.1. Stage 1: Frequency domain Energy Detection

Let $Y(k)$, $(k \in 1,\ldots,N_{fb})$ be the DFT of received signal samples in time domain, $y(n)$, $(n \in 1,\ldots,N_s)$, where N_{fb} and N_s represents the computed frequency bins and the acquired samples number, respectively.

In this paper, the value of N_s is fixed to 2401, in order to have a 20 kHz resolution over a 48 MHz span. Such resolution value is suitable for sensing purposes in 802.22 framework.

The obtained spectrum samples are divided into subsets, representing the sub–band segmentation of continuous spectrum analysis. The sub–sets' size has been chosen as uniform,in order to keep low the computational burden of the entire method, and the number of obtained sub–bands (M) is the result of three imposed constraints:

- having at least 30 samples per sub–band, so that theory deriving from the Central Limit Theorem (CLT) can be applied;
- sub–band width small enough to detect also narrow–band users, such as wireless microphones.
- finding the optimal trade–off between computational burden and achievable performance.

For each sub–band, a BHT testing different conditions for received signal can be applied:

$$Y_m(k) = \begin{cases} S_m(k) + W_m(k), & \text{under } H_m^1 \\ W_m(k), & \text{under } H_m^0 \end{cases}, \qquad (2)$$

where the following notation has been used:

- $S_m(k)$ is the frequency spectrum of the transmitted signal;
- $W_m(k)$ is the DFT of the additive white Gaussian noise;
- H_0 and H_1 are hypothesis about the presence of user signals, as described in Section 2.

It is easy to prove that: $W_m(\cdot)$, $S_m(\cdot)$ are vectors of independent and identically distributed (i.i.d.) realizations of a complex Gaussian random process [31].
In particular:

$$W_m(k) \sim \mathcal{CN}(0, \sigma_w^2), \qquad (3)$$

since its time–frequency transform is a linear and unitary operation, not modifying the random process distribution;

$$S_m(k) \sim \mathcal{CN}(0, \sigma_{s,m}^2), \qquad (4)$$

since the method does not include any demodulation of the received signal and, consequently, independence hypothesis can be still considered valid.

By considering the samples (N) in the m_{th} sub–band, it is possible to obtain the following computation formulas.

Starting from the (3) and (4), it is possible to obtain the distribution of received signal $Y_m(k)$, reported in (5).

$$\begin{cases} Y_m(k) \sim \mathcal{CN}(0, \sigma_{s,m}^2 + \sigma_w^2) & \text{under } H_1 \\ Y_m(k) \sim \mathcal{CN}(0, \sigma_w^2) & \text{under } H_0 \end{cases}. \qquad (5)$$

Following Neyman–Pearson approach, and considering $\vec{Y_m}$ as the vector containing all samples of Y in the m_{th} sub–band, it is possible to evaluate the likelihood ratio as follows:

$$T_m(\vec{Y_m}) = \frac{p(\vec{Y_m}|H_1)}{p(\vec{Y_m}|H_0)} \lessgtr \gamma_m, \tag{6}$$

where γ_m is a suitable threshold to be determined in the following, while $p(\vec{Y_m}|H_1)$ and $p(\vec{Y_m}|H_0)$ are the conditional probability density functions of $\vec{Y_m}$ under the hypotheses of noise only (H_0) or signal plus noise (H_1) channel conditions.

Therefore, the test statistic ($T_m(\vec{Y_m})$) can be computed as:

$$T_m(\vec{Y_m}) = \frac{\prod_{k=1}^{N} \frac{1}{\pi(\sigma_{s,m}^2+\sigma_w^2)} e^{-\frac{|Y_m(k)|^2}{(\sigma_{s,m}^2+\sigma_w^2)}}}{\prod_{k=1}^{N} \frac{1}{\pi(\sigma_w^2)} e^{-\frac{|Y_m(k)|^2}{(\sigma_w^2)}}}. \tag{7}$$

By computing the products, a further formulation is:

$$T_m(\vec{Y_m}) = \frac{\frac{1}{[\pi(\sigma_{s,m}^2+\sigma_w^2)]^N} e^{-\frac{1}{(\sigma_{s,m}^2+\sigma_w^2)} \sum_{k=1}^{N} |Y_m(k)|^2}}{\frac{1}{[\pi(\sigma_w^2)]^N} e^{-\frac{1}{(\sigma_w^2)} \sum_{k=1}^{N} |Y_m(k)|^2}}. \tag{8}$$

The ratio between quantities in (8) can be rewritten as:

$$T_m(\vec{Y_m}) = \left(\frac{\sigma_w^2}{\sigma_{s,m}^2 + \sigma_w^2}\right)^N e^{\left(\frac{1}{\sigma_w^2} - \frac{1}{\sigma_{s,m}^2+\sigma_w^2}\right) \sum_{k=1}^{N} |Y_m(k)|^2} \lessgtr \gamma_m. \tag{9}$$

Let us simplify the (9) by defining:

$$\alpha = \left(\frac{\sigma_w^2}{\sigma_{s,m}^2 + \sigma_w^2}\right)^N. \tag{10}$$

Furthermore, by applying natural logarithm to both sides of eqn. (9), it is possible to obtain:

$$\frac{\sigma_{s,m}^2}{\sigma_w^2(\sigma_{s,m}^2 + \sigma_w^2)} \sum_{k=1}^{N} |Y_m(k)|^2 \lessgtr ln(\frac{\gamma_m}{\alpha}) = \hat{\gamma}_m. \tag{11}$$

One more constant quantity can be renamed as β:

$$\beta = \frac{\sigma_{s,m}^2}{\sigma_w^2(\sigma_{s,m}^2 + \sigma_w^2)}. \tag{12}$$

Thus, the test statistic assumes the following simple formulation:

$$T_m(\vec{Y_m}) = \sum_{k=1}^{N} |Y_m(k)|^2 \lessgtr \frac{\hat{\gamma}_m}{\beta} = \bar{\gamma}_m. \tag{13}$$

The summation of squared modules of received samples can be decomposed in its mathematical formulation as:

$$T_m(\vec{Y_m}) = \sum_{k=1}^{N} \left[\left(Re\{Y_m(k)\}\right)^2 + \left(Im\{Y_m(k)\}\right)^2\right]. \tag{14}$$

Both the real and imaginary parts of $Y_m(k)$ are distributed as $\mathcal{N}(0, \frac{\sigma^2}{2})$, where the value of σ^2 is:

$$\begin{cases} \sigma^2 = \sigma_{s,m}^2 + \sigma_w^2 & \text{under } H_1 \\ \sigma^2 = \sigma_w^2 & \text{under } H_0 \end{cases}. \tag{15}$$

It is possible to standardize such variables and obtain:

$$T_m(\vec{Y_m}) = \frac{\sigma^2}{2}\left\{ \sum_{k=1}^{N} \left(\frac{Re\{Y_m(k)\}}{\frac{\sigma}{\sqrt{2}}}\right)^2 + \sum_{k=1}^{N} \left(\frac{Im\{Y_m(k)\}}{\frac{\sigma}{\sqrt{2}}}\right)^2 \right\}. \tag{16}$$

At this stage, each element of the summations is a standard normal distribution ($\mathcal{N}(0, 1)$) and each summation is a chi–square distribution with N degrees of freedom.

Therefore, the whole test statistic T_m is:

$$T_m \sim \frac{\sigma^2}{2}\chi^2(2N). \tag{17}$$

In further details, the test statistic (T_m) has the following possible distributions:

$$\begin{cases} T_m \sim \frac{\sigma_{s,m}^2+\sigma_w^2}{2}\chi^2(2N) & \text{under } H_1 \\ T_m \sim \frac{\sigma_w^2}{2}\chi^2(2N) & \text{under } H_0 \end{cases}. \tag{18}$$

.

If the number of samples (N) is large enough (typically greater than 30), the distributions expressed in (18) can be approximated with Normal distributions as follows:

$$\begin{cases} T_m \sim \mathcal{N}(N(\sigma_{s,m}^2 + \sigma_w^2), N(\sigma_{s,m}^2 + \sigma_w^2)^2) & \text{under } H_1 \\ T_m \sim \mathcal{N}(N\sigma_w^2, N\sigma_w^4) & \text{under } H_0 \end{cases}. \tag{19}$$

From distributions in (19), detection and false alarm probability can be computed in closed form as:

- Probability of detection (P_d):

$$P_{d,m} = P(T_m > \bar{\gamma}_m|H_1) = Q\left(\frac{\bar{\gamma}_m - N(\sigma_{s,m}^2 + \sigma_w^2)}{\sqrt{N}(\sigma_{s,m}^2 + \sigma_w^2)}\right); \tag{20}$$

- Probability of false alarm (P_{fa}):

$$P_{fa,m} = P(T_m > \bar{\gamma}_m|H_0) = Q\left(\frac{\bar{\gamma}_m - N\sigma_w^2}{\sqrt{N}\sigma_w^2}\right). \tag{21}$$

From such equations and, in particular, from P_{fa} expression (21), it is possible to compute the value for the threshold $\hat{\gamma}_m$:

$$\hat{\gamma}_m = \sigma_w^2[\sqrt{N}Q^{-1}(P_{fa,m}) + N]. \qquad (22)$$

In eqns. (20), (21), (22) the subscript m refers to the quantity evaluated for the m_{th} sub–band, while $Q(\cdot)$ and $Q^{-1}(\cdot)$ are the tail distribution function of the standard normal distribution and its inverse, respectively.

Therefore, the γ_m value can be calculated just once at the beginning of sensing phase, thus reducing the computational load of the algorithm. Moreover, if the false alarm rate can be kept constant for all sub–bands, i.e. the same performance level is targeted along the analyzed spectrum, the number of thresholds is reduced to a unique value. Furthermore, in (22), a fundamental parameter is the noise variance, i.e. σ_w^2. In the proposed method, it is computed at the beginning and periodically updated by acquiring a surely vacant channel, as the ones that exist for regulatory purposes in many world countries (e.g. in USA, channel 37), differently from other methods where it is assumed to be known *a priori*.

Main operations performed for Stage 1 are reported in Fig. 1. The output of such Stage is a M–sized binary vector, whose i_{th} component is set to "1" is the i_{th} sub–band is detected as occupied.

3.2. Stage 2: refinement method based on iterative approach

Since overall goal is to obtain efficient use of the spectral resource, the sub–band resolution could be poor and lead to useful band waste. The aim of Stage 2 is to refine outputs deriving from Stage 1, paying attention to "1_s" sub–bands, i.e. the spectrum portions declared as occupied by energy detector. Therefore, Stage 2 focuses on a very fine resolution, that is the frequency bin width obtained by transforming time signal samples through DFT. The proposed "Stage 2" is composed of a preliminary section and an iterative one. As for the preliminary section, the M–sized vector coming from the "Stage 1" is managed to make it suitable for the further operations. In detail, at first, contiguous bands (i.e. '1s' of the vector) are joint and starting and ending frequencies of these bands are estimated. Then suitable guard intervals, equal to half sub–band, are added at the beginning and at the end of each jointed interval. Finally, a smoothing filter (linear moving average) is applied to each joint interval to remove the noise from the trace.

Smoothing is a needed process, since such algorithm mainly works on the signal shape and noise ripples can heavily affect the detection process.

During the iterative phase, relevant levels of the smoothed trace are computed, i.e. signal top level (T_l) and noise floor (N_f). The former is computed as the mean value of local maxima, by considering as valid maxima only frequency bins whose amplitude is greater than the average value of the considered trace; the latter is similarly computed by taking into consideration the local minima. The noise proximity level (λ) is calculated according to (23).

$$\lambda = T_l - N_f. \qquad (23)$$

To establish whether N_f and T_l are significantly different to allow detection, a comparison with a detectability threshold ($\lambda_{det} = 3\sigma_w$) is performed. This value corresponds to a 99.7% of noise possible excursion. As a consequence if $\lambda > \lambda_{det}$, it can be supposed that there is a signal with a confidence level equal to 99.7% under the assumption of a Gaussian distribution of noise.

Only in this case, it is possible to determine the detection threshold, T_h, defined as:

$$T_h = \alpha T_l + \beta N_f \qquad (24)$$

In this work, α and β have been both set to 0.5.

By comparing the amplitude of each frequency bin with the threshold T_h, the occupied bandwidth is defined as:

$$f_{bi} \in Occ(B) \quad \text{if} \quad Y(f_{bi}) > T_h, \qquad (25)$$

where f_{bi} is a i_{th} discrete frequency bin, and $Occ(B)$ is the set of occupied bins.

After having checked all frequency bins delivered to Stage 2 analysis, adjacent bins belonging to the set ($Occ(B)$) are joint and considered occupied as a whole bandwidth. Spurious bins, passing the threshold check but being isolated, are rejected and considered as outliers. The so–obtained occupied bands undergo the normalization process, representing the last task of the iterative step. Such operation consists of replacing the amplitude of frequency bins belonging to the occupied bands with N_f value. In this way, high power users are detected during the first iterations (T_l is their top value), whilst weakest users can be detected in the following iterations, when the former have been normalized with estimated noise level. The detection of more powerful users will affect the computation of T_l level in the next iteration, since local maxima belonging to detected user signals are moved to have N_f value, due to the normalization process. Therefore, while N_f will remain pretty constant, since it especially depends of noise samples, T_l level will decrease iteration by iteration. Such trend

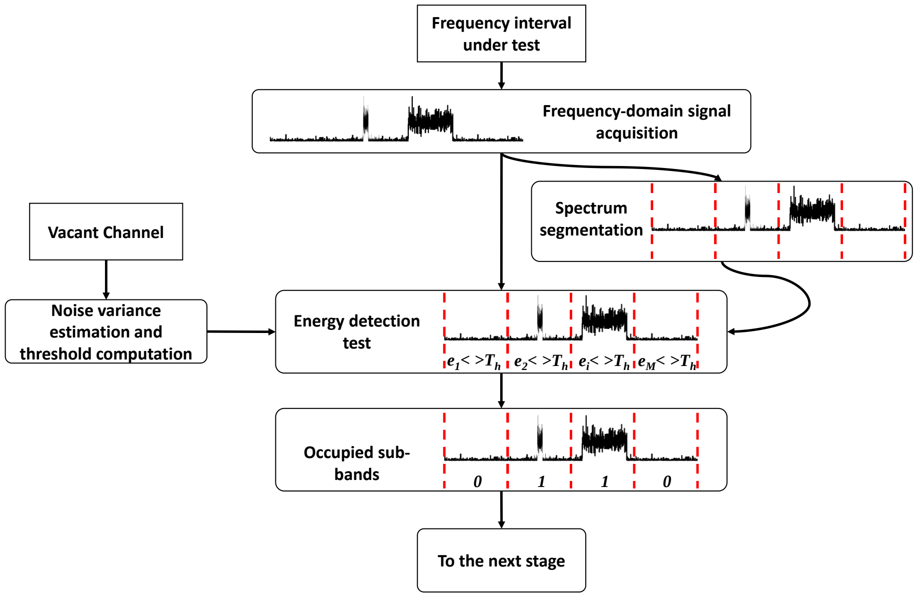

Figure 1: Block Diagram of Stage 1's main operations.

will lead the λ value to be very close to λ_{det}, thus not allowing to overcome the detectability threshold. In such condition, the algorithm ends.

When Stage 2 outputs null vectors, for example when very low SNR conditions are considered, Stage 1 results are the final outputs.

3.3. Computational Complexity

The proposed method is composed of two stages. Stage 1 operations consist of: N–point Fast Fourier Transform (FFT), N square operations, M (M<N) summations of $\lceil N/M \rceil$ samples, M comparisons. Stage 2 operations for each iteration consist of : evaluation of minimum and maximum in a K–sized array ($K < N$); $K + 1$ comparisons and S ($S << M$) assignments for normalization process, where K is the number of bins delivered to stage 2 by the algorithm and S is the number of occupied frequency bins. Considering the aggregate algorithm, the most resource–demanding operation is FFT, that is widely known [32] having computational complexity equal to $O(NlogN)$, while other tasks are all upper–bounded by $O(N)$. Furthermore, even if more than one iteration is considered for Stage 2, the average number of iterations is quite small (2 in our experimental test) and it does not significantly affect the computational complexity, that remains upper–bounded by $O(N)$ as Stage 2 regards. Therefore, for an N–sized input array, the obtained computational complexity is $O(NlogN)$.

4. Performance Assessment

Performance evaluation has been carried out by considering the output of the figures of merit described in subsection 4.1 obtained in simulation and emulation environments.

Three different scenarios representing typical users communicating in TVWSs have been realized. In particular, DTV and WM signals are considered in the analyzed frequency interval.

First scenario represents a DVB–T user in VHF band 174–222 MHz, having a 7 MHz bandwidth. Second and third scenarios are, instead, focused on UHF band 494 – 542 MHz and represent a situation of two simultaneously transmitting 8 MHz DVB–T users and a 200 kHz WM within a vacant TV channel, respectively.
Such scenarios have been tested for several channel conditions, expressed in terms of SNR. The considered SNR range is $\{-20 + 5k, 0 \leq k \leq 4\}$.

A snapshot of the acquired spectra is reported in Fig. 3 , where the considered scenarios are depicted in various SNR conditions, which are obtained by locking Noise Power to a fixed typical value ($\sigma_w^2 = -86.5$ dBm) and adjusting signal power to get the required ratio.
Moreover, for each channel conditions, 1000 repeated trials have been performed in order to give statistical relevance to the test.
As concerns Stage 1, different values for P_{fa}, ranging from 0% to 10%, have been tested and a number of

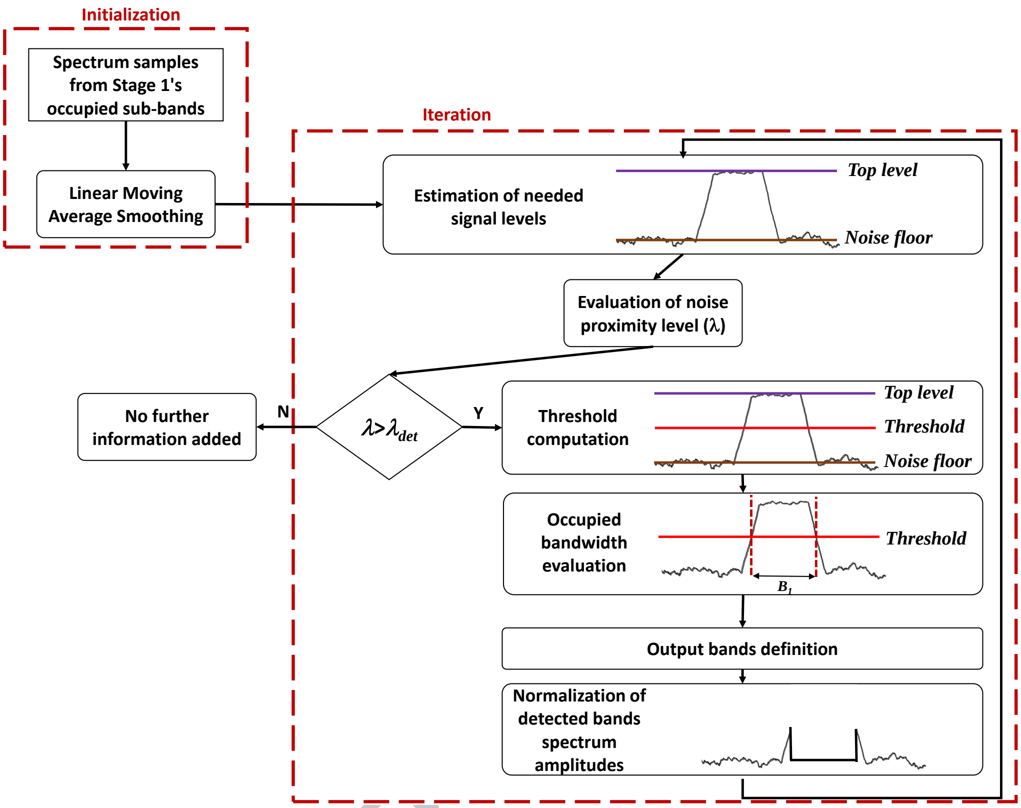

Figure 2: Block diagram of Stage 2's main operations.

Table 1: Description of proposed scenarios - frequency features.

Scenario ID	No. PUs	f_{c1} [MHz]	f_{c2} [MHz]	B_1 [MHz]	B_2 [MHz]
A	1	210	/	7	/
B	2	489	505	8	8
C	1	501	/	0.2	/

sub–bands equal to 33, each corresponding to 1.45 MHz width, has been chosen to obtain the described trade–off between capability to detect narrow–band signals and possibility to apply CLT [23].

The used frequency resolution is 20 kHz, corresponding to a total number of 2401 frequency bins in a 48 MHz span. Consequently, each sub–band is composed of a sub–set of about 70 bins, greater than the "30" required by CLT.

4.1. Figures of Merit

The considered performance indexes are:

- Mean Detected Bandwidth (MDB), defined as:

$$\mathrm{MDB}[\%] = \frac{1}{N_{sig}} \sum_{i=1}^{N_{sig}} \frac{\sum_{j=1}^{N_{b,i}} B_{j,i|H_1}}{B_{i|H_1}} 100\%, \qquad (26)$$

where:
  - N_{sig} is the total number of trials for each test conditions;
  - $N_{b,i}$ is the number of sub–bands (frequency bins) declared occupied by Stage 1 (Stage 2);
  - $B_{j,i|H_1}$ is the j_{th} detection in the i_{th} test within the H_1 zone (truly occupied bandwidth);
  - $B_{i|H_1}$ is the total bandwidth in H_1 zone.

This figure of merit has been designed to estimate the average detected bandwidth at each test

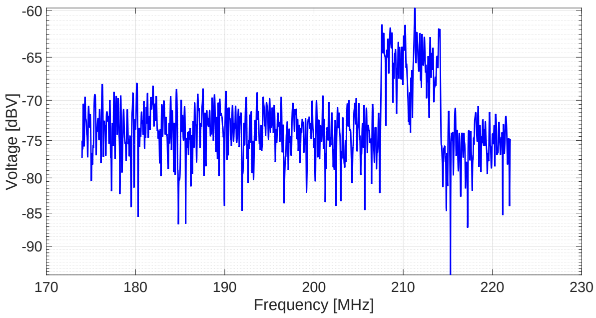

(a) Scenario A, SNR = 0 dB

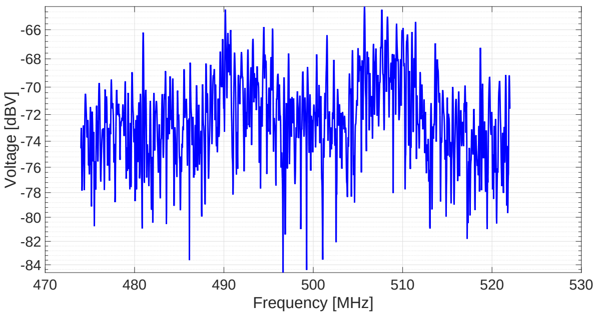

(b) Scenario B, SNR = – 5 dB

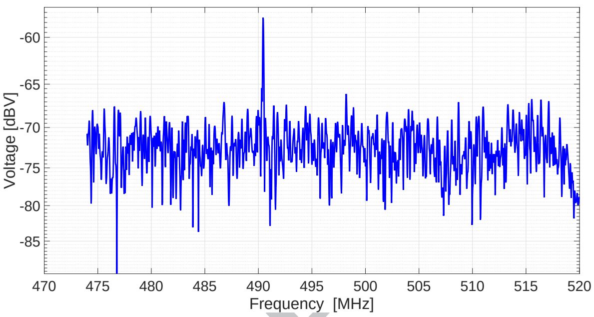

(c) Scenario C, SNR = – 10 dB

Figure 3: A snapshot of the acquired spectra for each considered scenarios.

with respect to the occupied zone. It is an important indication because it provides estimation information to the next stage designers for Cognitive Communications. The proposed figure of merit is quite new in Cognitive Radio field, but it derives from the measurement field experience and remarks a primary aspect when evaluating the capability of a spectrum sensing technique. It declares the percentage of the total bandwidth that the detector is able to reveal in average case, for a specific condition. Consequently, it provides important indications on the reliability and accuracy of the spectrum sensing method in estimating the actual occupied bandwidths, and such information can be advantageously employed in the next operating stage of Cognitive Radios (i.e. frequency agility) which is devoted to select the most proper frequency bands and modulation schemes to be adopted (during the transmission of the Secondary User) for minimizing the possibility of interfering with Primary Users.

- Probability of Detection (P_d) (Stage 1 only), defined as:

$$P_d = \frac{1}{N_{test}} \sum_{i=1}^{N_{test}} AND(B_{out,i}, Mask_{det}) \tag{27}$$

Since the Stage 1 of the proposed algorithm is based on a uniform sub-band division, its output is a binary array B_{out}, reporting "1" and "0" values where the energy test is passed or failed, respectively. To evaluate the capability to correctly reveal the occupied bandwidth, a same–size detection mask array ($Mask_{det}$) has been defined, reporting "1" and "0" values where signal plus noise or noise only are present, respectively. Therefore P_d evaluates the capabilities to detect the target signals, sub–band by sub–band, over the total number of tests (N_{test}). Consequently, P_d is an array, whose size is equal to number of adopted sub–bands.

Due to the typology of tested signals, each of them is usually wider than a single sub–band; therefore, it makes sense to subdivide the detected sub–bands into inner and outer (boundary) bands. The former are spectrum portions completely contained in the user signal bandwidth, while the latter are the first and the last sub–bands, that contain only the tails of the user signal spectrum. Stemming from such statement, two different P_d evaluations are proposed, by processing the P_d array defined in eq. 27.

$$P_{d,in} = \frac{\sum_{j=start\_index}^{stop\_index} P_d(j)}{stop\_index - start\_index + 1}; \tag{28}$$

$$P_{d,out} = \frac{P_d(start\_index - 1) + P_d(stop\_index + 1)}{2}. \tag{29}$$

In eq. 28, the average value of P_d results in inner bands is evaluated. This is obtained by considering *start_index* and *stop_index* as the first and last indexes of inner sub–bands. In scenarios reported in Table 2, user signals are always simulated to occupy an inner zone of the analyzed spectrum, therefore it is always possible to define boundary bands, over which the $P_{d,out}$ is computed according to eq. 29.

Probability of detection (P_d) can be evaluated only for stage 1 in the proposed scheme, since stage 2 has a customized detection algorithm, that is not based on classical binary hypothesis testing.

Performance results are presented in terms of MDB% versus the imposed False Alarm Probability (P_{fa}), that represents a degree of freedom of the presented method, and ROC curves (P_d vs P_{fa}).

4.2. Preliminary performance assessment in simulation environment

A preliminary analysis, aimed at verifying the behavior of the proposed method in a controlled environment and discovering the target performance indexes, has been carried out performing several numerical tests applying the method to simulated signals. To this aim, Scenario A has also been tested in simulation environment, and its results are reported in Figs. 4 – 7. In such figures, the behaviors of P_d and MDB versus SNR and P_{fa} are shown.

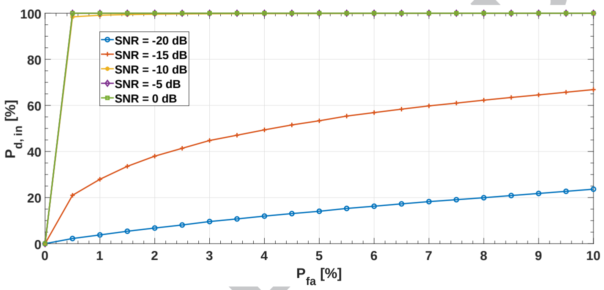

Figure 4: ROC curve for inner sub–bands $P_{d,in}$ vs P_{fa} at various SNRs.

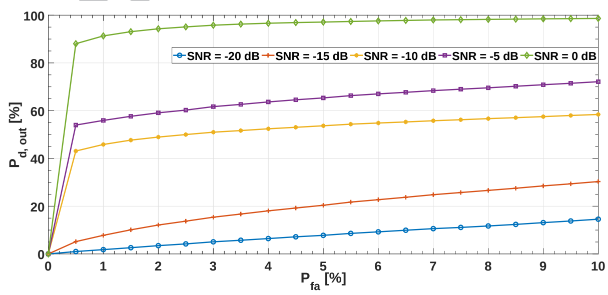

Figure 5: ROC curve for outer sub–bands $P_{d,out}$ vs P_{fa} at various SNRs.

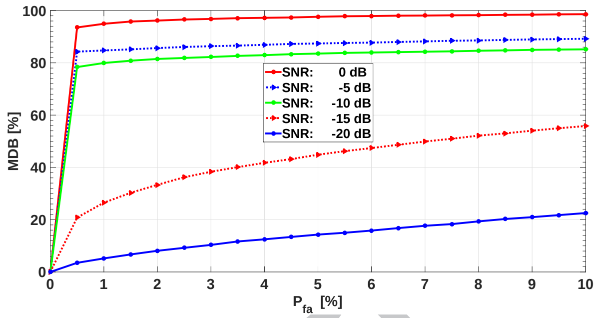

Figure 6: Scenario A - Stage 1 results.

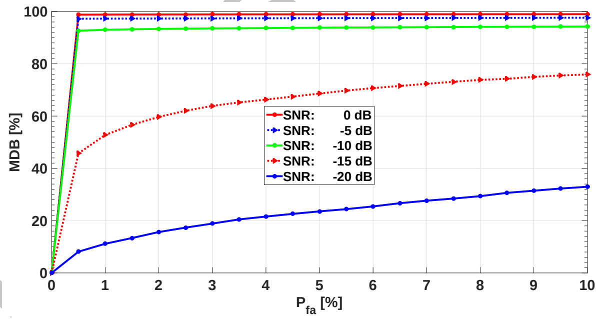

Figure 7: Scenario A - Overall results.

In particular, the ability of the proposed method to detect occupied bandwidth is tested with Stage 1 and its performance is reported in Figs. 4–5, while the capability to correctly measure the occupied spectrum is devoted to Stage 2 and its results are depicted in Fig. 7. To highlight the benefit introduced by the Stage 2, also Stage 1 MDB vs P_{fa} is reported in Fig. 6. As explained in subsection 4.1, P_d results are reported in terms of inner (see Fig. 4) and outer (see Fig. 5) detection ($P_{d,in}$ and $P_{d,out}$, respectively). Results show that, in inner bands case, $P_{d,in}$ values achieve 100% for SNRs > -15 dB, while for lower SNR, the increasing trend with respect to P_{fa} is appreciable but the method achieves lower $P_{d,in}$ values, upper–bounded by 66% and 24% for SNRs equal to -15 dB and -20 dB, respectively. The observation of Fig. 5 allows to understand how the boundary bands suffer worse detection performance because the occupancy percentage of those sub–bands by user signal is limited and the computed energy is often too low to pass the detection test. That is the reason why Stage 2 is employed, since it allows to refine the signal boundaries, especially acting on the rising and falling edges of the signal spectrum.

In terms of MDB, it is possible to distinguish Stage 1 results (Fig. 6) and Stage 2 results (Fig. 7). MDB trend is always increasing with the SNR. In particular,

Table 2: MDB Comparison in Scenario A - simulation case.

SNR [dB]	-20		-15		-10		-5		0	
P_{fa} [%]	1	10	1	10	1	10	1	10	1	10
Stage 1 MDB [%]	5.2	22.5	26.5	55.8	79.9	85.2	84.7	89.2	94.9	98.6
Stage 2 MDB [%]	11.1	32.9	52.7	75.9	93.1	94.3	97.2	97.6	98.8	98.9

by observing Fig. 6, and paying attention at a particular P_{fa} value (e.g. 5%), MDB obtained results range from 15% @ SNR = -20 dB to 98% @ SNR = 0 dB. Furthermore, the increase of imposed P_{fa} generates a further performance improvement. This phenomenon is more evident when low SNRs are considered, where the imposition of a P_{fa} ranging from 0.5% to 10% leads to a clear increase of the mean detected bandwidth (e.g. in Fig. 6, SNR = −20 dB, MDB = 4 % @ P_{fa} = 0.5 % towards MDB = 22 % @ P_{fa} = 10 %). Considering obtained numerical bounds, Stage 1 results show MDB values higher than 80% for any SNR > -15 dB. In case of worse SNRs, MDB is generally lower than 60%. By comparing Stage 1 and Stage 2 results, it is possible to note a general increasing of MDB values for all considered SNRs. As an example, let us consider two specific P_{fa} points (e.g. 1% and 10%). In this cases, obtained MDBs, reported in Tab. 2, describe the actual improvement obtained by adding Stage 2 to the Energy Detector algorithm. In any SNR condition, the overall sensing method performs better than Stage 1 only. Particularly, for lower SNRs the obtained enhancement is relatively greater than higher SNRs case.

4.3. Experimental Set–Up

The target performance, obtained for Scenario A in simulation environment, is the starting point for the extensive assessment of the proposed method through the use of scenarios realized by a laboratory set-up, containing real instrumentation for generating and acquiring the test scenarios.
To this aim, a measurement station, depicted in Fig. 8, has been designed and implemented. It includes:

(i) a RF vector signal generator, model Agilent Technologies^{TM} N5182A (100 kHz–6 GHz output frequency range);

(ii) a Tektronix^{TM} RSA6114A Real–time spectrum analyzer (9 kHz–14 GHz input frequency range, 14–bits ADC);

(iii) a standard PC as control unit for the instruments automatic operation through GPIB and Ethernet interfaces.

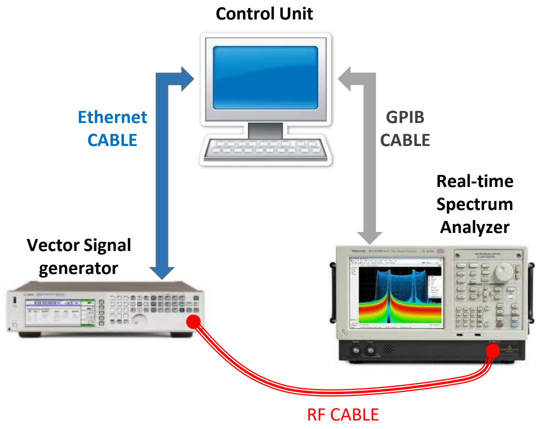

Figure 8: A sketch of the measurement station adopted for the experimental validation of the proposed method.

In particular, the signal generator has been programmed through its Ethernet interface and by using the software Agilent Signal Studio for Digital Video N7623B with the aim of generating scenarios reported in Table 1, representing typical users in the analyzed frequency interval. The generator allows emulating an AWGN channel with an imposed SNR (same values adopted in simulation environment were considered). The RSA has been used to acquire the signals that are successively processed by the proposed sensing method. The control software has been developed in LabView environment and allows to communicate with the instrument through GPIB interface. Main RSA setting parameters considered during the experimental tests are:

- Detector: CISPR Peak;
- Filter shape: CISPR;
- Function: AVG (V_{RMS});
- SPAN: 48 MHz;
- Resolution Bandwidth: 20 kHz;
- Trace points: 2401.

4.4. Experimental Results

Obtained performance in emulated scenario is reported in Figs. 9–14. The same figure of merit has been used

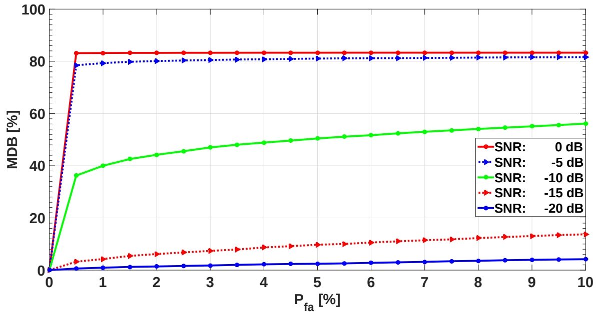

Figure 9: Scenario A - Stage 1 results - emulation.

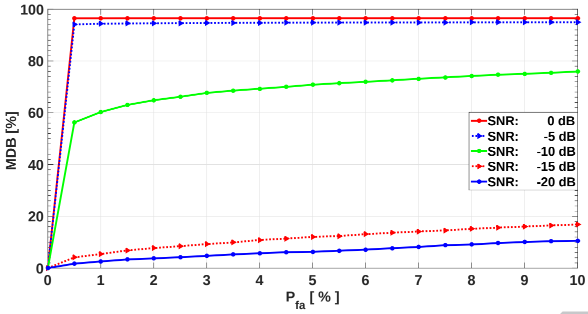

Figure 10: Scenario A - Overall results - emulation.

to estimate the detection capability of the method. Results depicted in Figs. 9, 10 can be compared with those obtained in simulation environment (Figs. 6, 7), regarding Scenario A. The effect of actual hardware, adding quantization noise and other acquisition non–idealities, is particularly remarkable for any tested SNR, both in Stage 1 and Stage 2 results. It is possible to quantify the performance gap in about 10% in medium case. In emulation case, the addition of Stage 2 is strictly necessary, for Scenario A, since it allows to achieve good performance level, by compensating the effect of real signal generation through the further processing stage.

Best results are obtained for higher SNRs, when MDB in the overall computation achieves values greater than 90%, for SNR > -10 dB and any imposed P_{fa} value. Lower SNRs show a good increasing trend versus P_{fa}.

As for Scenario B, situation gets worse because of two simultaneously transmitting users in the frequency span of interest. Since the SNR condition is imposed as a wide–band setting, the real experienced SNR by each of the user is less than the one obtained in Scenario A, where a single user is present.

This scenario has been carried out to further stress the method with respect to difficult operating conditions in the channels of interest. The MDB values, displayed in Figs. 11, 12, are mean values of estimated bandwidth percentage for the considered users. Therefore, even for higher SNRs (0 dB, -5 dB), MDB results are around 65% for Stage 1 and 85% after Stage 2 application. Similar performance is obtained for lower SNR, resulting in a reliable detection down to -10 dB. Even for Scenario B, the introduction of a second refinement stage brings to strongly improve obtained performance levels.

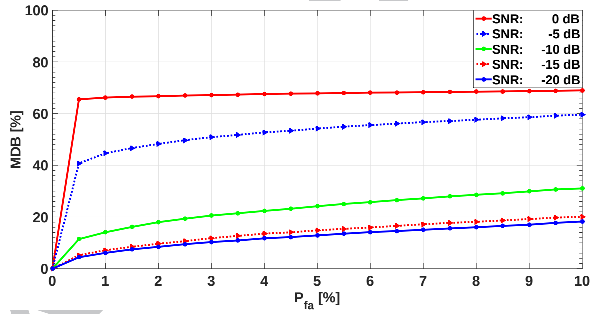

Figure 11: Scenario B - Stage 1 results - emulation.

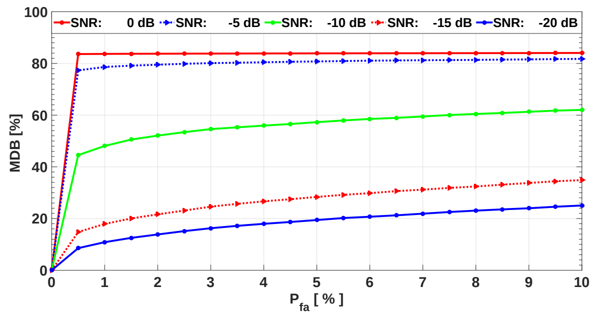

Figure 12: Scenario B - Overall results - emulation.

In Scenario C, a wireless microphone case is presented. In this situation, the 200 kHz bandwidth is an improvement factor in terms of experienced SNR towards the wide–band imposition. This motivation leads to a strong improvement of the MDB index, by making the detection reliable down to SNR $= -20$ dB, where after Stage 2 processing an average MDB = 75% is obtained.

In this case, the application of second Stage to the sensing method does not carry out the same improvement ratios seen for Scenario A and B. SNRs > -20 dB always allow to have MDB close to 100% for every tested P_{fa} value.

The SNR is surely the most influencing parameters for obtaining reliable detection of different users in TVWSs. Adding further computation effort has led to

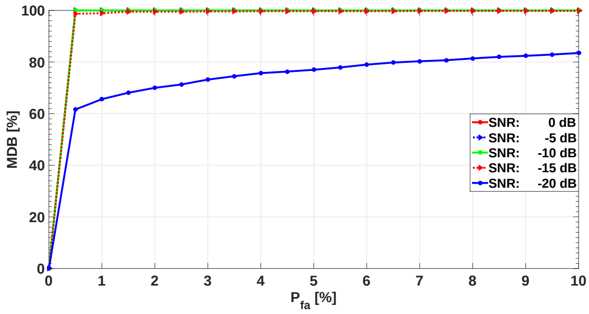

Figure 13: Scenario C - Stage 1 results - emulation.

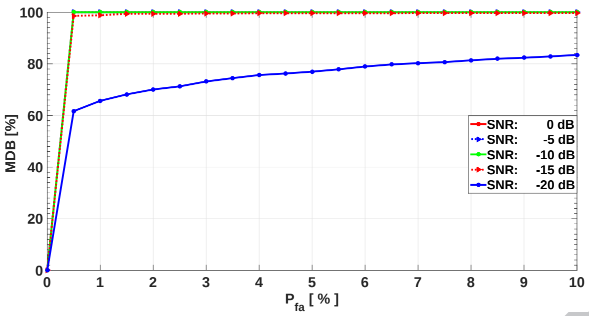

Figure 14: Scenario C - Overall results - emulation.

an important improvement when Stage 1 performance was damaged by bad channel conditions. The emulation environment is a further influencing factor and its effect is particularly clear when performance related to the same scenario (A) is compared. Therefore, the most the method works on real operating conditions, the best the application of a two–stage to the sensing, since the Energy Detector (Stage 1) only is not able to guarantee adequate detection capabilities in difficult scenarios.

5. Comparison against another two–step energy detection scheme

The proposed method is characterized by two stages, as others that are in literature. Particularly interesting is the analysis and comparison with the method proposed in [33]. Several reasons allow to accomplish the comparison: both of them start from classical definition of energy detection, evaluate the behavior of their performance with varying SNR regime, claim to overperform standard energy detection and are two–stage featured, with optional second stage. Some figures of merit could be adopted to perform the comparison. Some of them are related to the metrological feature of the methods (accuracy, resolution, sensitivity), while others could be related to the applicability of the methods on real platforms and in real applications (detection time, computational complexity,etc). In this paragraph both these aspects are considered. To achieve the goal, common performance index (P_d) has been computed for first stage only in case of proposed method. A first important difference has to be declared at this point: while in [33], the channelization is assumed to be known and the energy detection is performed in time domain, focused only on the channel of interest, the algorithm proposed in this paper is completely blind in terms of knowledge about signal position and bandwidth, although it is customized to work in TVWS context.

Therefore, while it is clear and unequivocal the P_d definition when a single channel is sensed, in a blind wide–band energy detection case, different definitions can be achieved. For the comparison the definitions, reported in eqs. 27– 29, are adopted.

Results provided in Table 3 are obtained by imposing a constant false alarm rate $P_{fa} = 10\%$. To have knowledge about the $P_{d,in}$ and $P_{d,out}$ behavior vs P_{fa} and SNR, full ROC curves are provided in Figs. 4–5, in case of Scenario A, that is the same one adopted for comparison. Since Stage 1 is related to energy test in independent sub–bands, the choice of Scenario A instead of Scenario B does not affect statement validity.

Obtained compared results highlight two different issues: as for inner bands, the proposed method overcomes performance obtained in [33]. As regards outer bands, results got worse and therefore the adoption of the Stage 2 is intended to improve detection capability by measuring the actual occupied signal spectrum, through a bin–based detection scheme. In particular, the worsening of performance in outer bands is due to the uniform sub–band division, causing that tails of the signal occupy only a very small portion of each outer bands (either the starting rising edge or the ending falling one), not resulting sufficient for energy test passing. Since Stage 2 adopts the policy to analyze the Stage 1 occupied sub–bands and takes guard intervals before and after such bands, such results can be improved by analyzing the spectrum bin by bin, as Stage 2 does. The improving effect is shown in Section 4. Therefore the

Table 3: Comparison between proposed and compared approach on common SNR regimes

Method\ SNR	−10 dB	−5 dB	0 dB
Proposed Method ($P_{d,in}[\%]$)	99	100	100
Proposed Method ($P_{d,out}[\%]$)	58	72	99
Comparison Method (P_d)	40	92	100

overall comparison states that the proposed method performs better than [33] sub–bands are contained in the user signal and, for outer bands case, Stage 2 is able to fill the gap by analyzing signal tails bin by bin. In terms of applicability to general case a uniform sub–band division, as the proposed method carries out, allows to detect several typologies of signals and it is independent of the channelization and signal bandwidths. It is an important advantage with respect to various typologies of energy detection based system, where channelization is usually known *a priori* and only specific signals can be detected at a time. In terms of sensitivity, the proposed method is able to detect signals down to -15 dB corresponding, considering a typical noise level of -95 dBm for a real instrument such as a Software Defined Radio, to a detection sensitivity equal to -110 dBm. Compared methods and other present in literature do not provide this kind of information and SNR = $-$ 10 dB is usually a typical lower bound for performance assessment. Furthermore, as frequency resolution regards, standard energy detection and also the one proposed in [33] present frequency resolution equal to the channel bandwidth to be detected since the detection phase is carried out in time domain and only a band–pass filter is adopted. On the contrary, the proposed approach allows to have a frequency resolution equal to the sub–band for stage 1 and to the frequency bin for Stage 2. To include numerical values, the sub–band width is set to 1.4 MHz and the frequency bin has a 20 kHz bandwidth. Finally, as for computational complexity it is reported in Section 3.3 and it is mainly due to FFT process. All sensing methods adopting a frequency domain approach are lower–bounded by this complexity value. As for detection time, the authors in [33] claim to have reduced the detection time thanks to an optimization in the number of needed samples. The proposed approach is modular in terms of detection time, as explained in the introduction, and it can be reduced or extended according to the needs a specific application can have.

6. Conclusions

This paper has presented a spectrum sensing method for dynamic spectrum access in cognitive radio applications. It has been designed for operating in VHF and UHF bands where TVWSs could be found and then exploitable by SUs for enhancing the overall efficiency in spectrum usage.

According to different needs of the target application in terms of computational efforts and accuracy level in the detection of actual bandwidths occupied by PUs, the proposed method is based on two sequential stages, the first one employing an energy detection in frequency domain able to quickly reveal the sub bands occupied by PUs, and the second one which analyzes only the sub–bands declared as occupied (by Stage 1) for refining and improving the frequency resolution and accuracy in the PU detection. Dependently on the accuracy and promptness levels required by the context, the user has the possibility to select to carry out a fast analysis (less accurate) or a slow analysis (more accurate).

To evaluate the method performance, a suitable figure of merit, namely the Mean Detected Bandwidth (MBD), has been defined for evaluating the accuracy of the method in correctly measuring the PU bandwidth. An experimental campaign has been carried out by varying the target False Alarm probability (from 0.5% up to 10%) and the SNR (from -20 dB up to 0 dB) when the method is applied on signal coming from a signal generator and acquired by a real Radio Frequency Data acquisition system.

In particular, the benefits of Stage 2 on the overall performance has been verified on several emulated scenarios compliant with the contexts defined in the IEEE 802.22 standard. In a more detail, the second stage allows improving the MDB of about 15% (for scenarios A and B).

Furthermore, for $\mathrm{SNR} > -10\,\mathrm{dB}$, the two–stage method warrants a MDB > 80% whatever be the scenario and the selected target P_{fa}. These features are very promising for an implementation on real devices operating in DSA communications such as SDR.

References

[1] ITU, ICT Facts and Figures 2017 (July 2017).

[2] R. Thanki, Measuring the Local Impact of the TV WhiteSpace Broadband (2015).

[3] A. Mody, G. Chouinard, S. J. Shellhammer, M. Ghosh, D. Cavalcanti, Cognitive Wireless Regional Area Network Standard, John Wiley & Sons, Inc, 2015, pp. 551–603. doi:10.1002/9781119057246.ch23.

[4] FCC, Spectrum Policy Task Force Report, ET. Docket No. 02-135 (November 2011).

[5] T. Taher, R. Bacchus, K. Zdunek, D. Roberson, Long-term spectral occupancy findings in Chicago, in: proc. 2011 IEEE Symposium on of New Frontiers in Dynamic Spectrum Access Networks (DySPAN), 2011, pp. 100–107. doi:10.1109/DYSPAN.2011.5936195.

[6] T. Taher, R. Attard, A. Riaz, D. Roberson, J. Taylor, K. Zdunek, J. Hallio, R. Ekman, J. Paavola, J. Suutala, J. Roning, M. Matinmikko, M. Hoyhtya, A. MacKenzie, Global spectrum observatory network setup and initial findings, in: proc. of 2014 9th International Conference on Cognitive Radio Oriented Wireless Networks and Communications (CROWNCOM), 2014, pp. 79–88.

[7] S. Barnes, P. J. van Vuuren, B. Maharaj, Spectrum occupancy investigation: Measurements in south africa, Measurement 46 (9) (2013) 3098 – 3112. doi:https://doi.org/10.1016/j.measurement.2013.06.010.

[8] J. Xue, Z. Feng, P. Zhang, Spectrum Occupancy Measurements and Analysis in Beijing, IERI Procedia 45 - 302, 2013 International Conference on Electronic Engineering and Computer Science (EECS 2013). doi:https://doi.org/10.1016/j.ieri.2013.11.042.

[9] A. A. Ayeni, N. Faruk, O. W. Bello, O. A. Sowande, S. O. Onidare, M. Y. Muhammad, Spectrum Occupancy Measurements and Analysis in the 2.4-2.7 GHz Band in Urban and Rural Environments, International Journal of Future Computer and Communication 5 (3) (2016) 142 – 147. doi:10.18178/ijfcc.2016.5.3.461.

[10] S. Jayavalan, H. Mohamad, N. M. Aripin, A. Ismail, N. Ramli, A. Yaacob, M. A. Ng, Measurements and Analysis of Spectrum Occupancy in the Cellular and TV Bands, Lecture Notes on Software Engineering 2 (2) (2014) 133 – 138. doi:10.7763/LNSE.2014.V2.110.

[11] IEEE, IEEE Standard for Information technology– Local and metropolitan area networks– Specific requirements– Part 22: Cognitive Wireless RAN Medium Access Control (MAC) and Physical Layer (PHY) specifications: Policies and procedures for operation in the TV Bands, IEEE Std 802.22-2011 (2011) 1–680doi:10.1109/IEEESTD.2011.5951707.

[12] NICT, Hitachi Kokusai Electric, World's First breakthrough Achieved for Long–Range Broadband Communications in TV White Space, press release.

[13] A. Mody, A. Saha, I. Reede, G. Miele, G. Cerro, IEEE 802.22/802.22.3 Cognitive Radio Standards: Theory to Implementation, Springer Singapore, Singapore, 2017, pp. 1–52. doi:10.1007/978-981-10-1389-8_54-1.

[14] IEEE, P802.22/D2 Draft Standard for Information Technology – Telecommunications and information exchange between systems Wireless Regional Area Networks (WRAN) – Specific requirements. Part 22.3: Spectrum Characterization and Occupancy Sensing, IEEE Std Draft 802.22.3 (2017) 1–106.
URL `https://mentor.ieee.org/802.22`

[15] L. Gonzales-Fuentes, K. Barbé, W. V. Moer, N. Björsell, Cognitive radios: Discriminant analysis for automatic signal detection in measured power spectra, IEEE Transactions on Instrumentation and Measurement 62 (12) (2013) 3351–3360. doi:10.1109/TIM.2013.2265607.

[16] D. Bao, L. D. Vito, S. Rapuano, A histogram-based segmentation method for wideband spectrum sensing in cognitive radios, IEEE Transactions on Instrumentation and Measurement 62 (7) (2013) 1900–1908. doi:10.1109/TIM.2013.2251821.

[17] M. Hamid, N. Björsell, W. V. Moer, K. Barbé, S. B. Slimane, Blind spectrum sensing for cognitive radios using discriminant analysis: A novel approach, IEEE Transactions on Instrumentation and Measurement 62 (11) (2013) 2912–2921. doi:10.1109/TIM.2013.2267456.

[18] W. A. Jerjawi, Y. A. Eldemerdash, O. A. Dobre, Second-Order Cyclostationarity-Based Detection of LTE SC-FDMA Signals for Cognitive Radio Systems, IEEE Transactions on Instrumentation and Measurement 64 (3) (2015) 823–833. doi:10.1109/TIM.2014.2357592.

[19] S. Yarkan, A generic measurement setup for implementation and performance evaluation of spectrum sensing techniques: Indoor environments, IEEE Transactions on Instrumentation and Measurement 64 (3) (2015) 606–614. doi:10.1109/TIM.2014.2355471.

[20] L. D. Vito, A review of wideband spectrum sensing methods for cognitive radios, in: 2012 IEEE International Instrumentation and Measurement Technology Conference Proceedings, 2012, pp. 2257–2262. doi:10.1109/I2MTC.2012.6229530.

[21] L. Angrisani, D. Capriglione, G. Cerro, L. Ferrigno, G. Miele, On Employing a Savitzky-Golay Filtering Stage to Improve Performance of Spectrum Sensing in CR Applications Concerning VDSA Approach, Metrology and Measurement Systems 23 (2) (2016) 295 – 308.

[22] L. Angrisani, D. Capriglione, G. Cerro, L. Ferrigno, G. Miele, Optimization and experimental characterization of novel measurement methods for wide-band spectrum sensing in cognitive radio applications, Measurement 94 (2016) 585–601. doi:https://doi.org/10.1016/j.measurement.2016.08.036.

[23] L. Angrisani, D. Capriglione, G. Cerro, L. Ferrigno, G. Miele, A dual step energy detection based spectrum sensing algorithm for cognitive vehicular ad hoc networks, in: 2015 IEEE International Instrumentation and Measurement Technology Conference (I2MTC) Proceedings, 2015, pp. 1622–1627. doi:10.1109/I2MTC.2015.7151522.

[24] D. Capriglione, G. Cerro, L. Ferrigno, G. Miele, The effect of ADC vertical resolution on the performance of an energy detection algorithm in cognitive radios, in: 2018 IEEE International Instrumentation and Measurement Technology Conference (I2MTC), 2018, pp. 1–6. doi:10.1109/I2MTC.2018.8409825.

[25] L. Angrisani, D. Capriglione, L. Ferrigno, G. Miele, Frequency agility in cognitive radios: A new measurement algorithm for optimal operative frequency selection, Measurement 82 (2016) 26 – 36. doi:https://doi.org/10.1016/j.measurement.2015.12.034.

[26] S. Geethu, G. Narayanan, A novel high speed two stage detector for spectrum sensing, Procedia Technology 6 (2012) 682 – 689, 2nd International Conference on Communication, Computing & Security [ICCCS-2012]. doi:https://doi.org/10.1016/j.protcy.2012.10.082.

[27] S. Maleki, A. Pandharipande, G. Leus, Two-stage spectrum sensing for cognitive radios, in: 2010 IEEE International Conference on Acoustics, Speech and Signal Processing, 2010, pp. 2946–2949. doi:10.1109/ICASSP.2010.5496149.

[28] Z. Li, H. Wang, J. Kuang, A two-step spectrum sensing scheme for cognitive radio networks, in: International Conference on Information Science and Technology, 2011, pp. 694–698. doi:10.1109/ICIST.2011.5765341.

[29] S. Suwanboriboon, W. Lee, A novel two-stage spectrum sensing for cognitive radio system, in: 2013 13th International Symposium on Communications and Information Technologies (ISCIT), 2013, pp. 176–181. doi:10.1109/ISCIT.2013.6645845.

[30] K. Srisomboon, A. Prayote, W. Lee, Two-stage spectrum sensing for cognitive radio under noise uncertainty, in: 2015 Eighth International Conference on Mobile Computing and Ubiquitous Networking (ICMU), 2015, pp. 19–24. doi:10.1109/ICMU.2015.7061022.

[31] Z. Quan, S. Cui, A. Sayed, H. Poor, Optimal Multiband Joint Detection for Spectrum Sensing in Cognitive Radio Networks, IEEE Trans. Signal Process. 57 (3) (2009) 1128–1140. doi:10.1109/TSP.2008.2008540.

[32] C. H. Papadimitriou, Optimality of the fast fourier transform, J. ACM 26 (1) (1979) 95–102. doi:10.1145/322108.322118.
URL `http://doi.acm.org/10.1145/322108.322118`

[33] M. Lai, S. Peng, X. Yang, L. Zhou, Fast two-step energy detection for spectrum sensing, Journal of Electrical and Computer Engineering 2015, (2015) 1–7. doi:10.1155/2015/591627.